Published in final edited form as:
Microcirculation. 2011 February ; 18(2): 85–101. doi:10.1111/j.1549-8719.2010.00057.x.

Characterization of Prox1 and VEGFR-3 expression and lymphatic phenotype in normal organs of mice lacking p50 subunit of NF-κB

Michael J. Flister, **Lisa D. Volk**, and **Sophia Ran**
Department of Medical Microbiology, Immunology, and Cell Biology, Southern Illinois, University School of Medicine, Springfield, IL

Abstract

Objective—Inflammation and Nuclear Factor-kappa B (NF-κB) are highly associated with lymphangiogenesis but the underlying mechanisms remain unclear. We recently established that activated NF-κB p50 subunit increases expression of the main lymphangiogenic mediators, vascular endothelial growth factor receptor-3 (VEGFR-3) and its transcriptional activator, Prox1. To elucidate the role of p50 in lymphatic vasculature, we compared lymphatic vessel density (LVD) and phenotype in p50 knockout (KO) and wild-type (WT) mice.

Methods—Normal tissues from KO and WT mice were stained for LYVE-1 to calculate LVD. VEGFR-3 and Prox1 expressions were analyzed by immunofluorescence and qRT-PCR.

Results—Compared with WT, LVD in the liver and lungs of KO mice was reduced by 39% and 13%, respectively. This corresponded to 25–44% decreased VEGFR-3 and Prox1 expression. In the mammary fat pad (MFP), LVD was decreased by 18% but VEGFR-3 and Prox1 expression was 80–140% higher than in WT. Analysis of p65 and p52 NF-κB subunits and an array of inflammatory mediators showed a significant increase in p50 alternative pathways in the MFP but not in other organs.

Conclusions—These findings demonstrate the role of NF-κB p50 in regulating the expression of VEGFR-3, Prox1 and LVD in the mammary tissue, liver, and lung.

Keywords

lymphatic vessels; nuclear factor-kappa B; p50; vascular endothelial growth factor receptor-3; Prox1

INTRODUCTION

The function of lymphatic vessels is important for proper immune cell transport [35], response to injury [55], homeostasis[53] and dissemination of tumor cells [28,61]. The formation of new lymphatic vessels, a process known as lymphangiogenesis, is a frequent event during embryogenesis but it is tightly regulated in adulthood. The key protein that mediates lymphangiogenesis is the vascular endothelial growth factor receptor (VEGFR)-3 [74]. This protein is expressed primarily on lymphatic endothelial cells (LECs) and is activated by growth factors VEGF-C and VEGF-D [3]. Activation of VEGFR-3 signaling

Address correspondence to: Sophia Ran, Department of Medical Microbiology, Immunology and Cell Biology, Southern Illinois University School of Medicine, 801 N. Rutledge, Springfield, IL, 62794-9626, USA. Phone: (217) 545–7026; Fax: (217) 545–7333; sran@siumed.edu.

increases LEC proliferation, migration, and survival [46,74], whereas blocking the VEGFR-3 pathway inhibits both inflammation-induced [5] and cancer-promoted [63] lymphangiogenesis.

Typically, acute inflammation does not elicit pro-lymphangiogenic response. However, chronic inflammation frequently induces new lymphatic vessels as has been described in malignancy [28,61] and those associated with arthritis [80], psoriasis [27,41], renal transplant rejection [40], chronic airway inflammation [5], inflammatory bowel disease [22], and peritonitis [20,37]. Inflammation is primarily mediated by transcription factors belonging to the NF-κB family that contains five subunits: p50 (NF-κB1), p65 (Rela), p52 (NF-κB2), RelB, and cRel [23]. All five NF-κB factors contain the Rel homology domain that mediates binding to the prototypic κB element typically present in the promoters of inflammation-responsive genes [73]. The most abundant NF-κB transcription factors are dimers containing p50/p50, p50/p65, or p65/p65 subunits [29,30] that regulate expression of more than 400 proteins implicated in inflammation [1], immunity [23], tumorigenesis [15], angiogenesis [81], and lymphangiogenesis [5,50].

Out of the two most abundant subunits of NF-κB family, p50 and p65, the former appears to play a more prominent role in inducing lymphangiogenesis and the normal development of the lymphatic system. This is primarily based on evidence demonstrating constitutive expression of p50 and its precursor protein p105 [64] in the murine lymphatic system and sharp elevation of its expression in response to inflammatory stimuli, TNF-α or LPS [5,37]. Both treatments have been shown to induce lymphangiogenesis [6,37], suggesting that NF-κB p50 might be required for this process. Consistent with this hypothesis, we recently showed in cultured LECs that p50 has a 10-fold higher transactivation potential than p65, and co-transfection of p50 and the VEGFR-3 promoter results in up to 100-fold activation of this promoter [20]. We also showed that p50 was one of the early factors up-regulated during inflammatory lymphangiogenesis in which its increase preceded induction of both VEGFR-3 and the formation of new lymphatic vessels [20].

Another protein coincidently up-regulated with p50 in the thioglycollate (TG) inflammatory model was the homeobox transcription factor, Prox1. This protein defines the lymphatic fate in early venous endothelial cells thus playing a pivotal role in development of embryonic lymphatic system [76,77]. The essential role of Prox1 in embryonic lymphangiogenesis suggests that it might play a similar pro-lymphangiogenic role in postnatal events. Indeed, we showed that the level of Prox1 expression rapidly and sharply increased in the earliest timepoints of inflammation preceding by several days both increased lymphatic expression of VEGFR-3 and genesis of new lymphatic vessels [20]. Moreover, we showed that Prox1 directly binds and activates the VEGFR-3 promoter suggesting that its early increase during inflammation is necessary for elevating VEGFR-3 expression [20]. This finding is in accord with multiple prior studies that showed positive correlation between increased Prox1 and VEGFR-3 expression levels in LEC and blood vascular endothelial cells (BEC) treated with inflammatory stimuli [20,32,48,56,59].

Taken together the evidence for the regulatory role of Prox1 in VEGFR-3 expression and our novel findings associating NF-κB p50, Prox1 and VEGFR-3, we hypothesized that the absence of NF-κB p50 might both suppress Prox1 and VEGFR-3 expression and attenuate formation of lymphatic vessels. We further hypothesize that if NF-κB p50 plays a role in the initial formation of lymphatic vessels, this might be reflected by reduced lymphatic vessel density (LVD) in normal organs of adult mice with genetically ablated NF-κB p50 (p50 KO). To test this hypothesis, we compared LVD in various organs of p50 KO mice with corresponding wild-type littermates (p50 WT). Unlike embryonically lethal deletion of NF-κB p65 [8], p50 KO mice survive to adulthood but with multifocal defects in response to

immune challenge [67]. Neither the blood nor lymphatic vascular phenotype of NF-κB p50 KO mice has been previously investigated. Therefore, the goal of this study was to compare LVD in different organs of p50 KO and WT mice and to correlate LVD with the expression levels of major pro-lymphangiogenic proteins, VEGFR-3 and Prox1. Comparison of LVD between WT and p50 KO mice revealed significantly reduced number of LYVE-1^+ vessels in the liver, lung, and in the equivalent of human breast tissue, the mammary fat pad (MFP). In the lung and the liver, this correlated with decreased levels of VEGFR-3 and Prox1 expression measured by qRT-PCR and immunofluorescence. These novel findings provide genetic evidence for the organ-specific role of NF-κB p50 in regulation of VEGFR-3 and Prox1 expression, and optimal lymphatic vessel density in several major normal organs of adult mice.

MATERIALS AND METHODS

Antibodies

Goat anti-mVEGFR-3 and anti-Prox1 antibodies were purchased from R&D Systems (Minneapolis, MN). Rabbit anti-mLYVE-1 and anti-Prox1 antibodies were purchased from AngioBio (Del Mar, CA). Secondary donkey anti-rabbit, anti-goat, and anti-rat antibodies conjugated with DyLight 488 or DyLight 549 were purchased from Jackson ImmunoResearch Laboratories (West Grove, PA).

Animals

Female B6129PF2/J (F2) ($p50^{+/+}$) and B6;129P2-Nfkb 1<tm 1 Bal> ($p50^{-/-}$) mice 4–6 weeks of age were obtained from the Jackson Laboratory (Bar Harbor, ME) and treated in accordance with institutional guidelines set by the Animal Care and Use Committee at Southern Illinois University School of Medicine. Mice were anesthetized with a mixture of ketamine (Fort Dodge Animal Health, Fort Dodge, Iowa), xylazine (Phoenix Scientific Inc., St. Joseph, Missouri) and sterile water. Prior to tissue harvesting, fully anesthetized mice were perfused with 5mM $CaCl_2$ solution. Harvested tissues were snap-frozen in liquid nitrogen and then fixed in Shandon Cryomatrix (Thermo Scientific, Waltham, MA) for cryostat sectioning.

Immunofluorescent staining

Frozen sections were fixed with acetone for 10 minutes, washed in PBST (pH 7.4, 0.1% Tween-20) for 10 minutes and incubated for 2 hours at 37°C with primary antibodies (diluted 1:100 in PBST containing 5 μg/ml BSA) against VEGFR-3, LYVE-1, Prox1, or MECA-32, followed by appropriate DyLight 488- or 549-conjugated secondary antibodies (diluted 1:100 in PBST containing 5 μg/ml BSA) for 1 hour at 37°C. Slides were mounted in Vectashield medium containing 4,6′-diamidino-2-phenylindole (DAPI) nuclear stain (Vector Labs, Orton Southgate, U.K.). Images were acquired on an Olympus BX41 upright microscope equipped with a DP70 digital camera and DP Controller software (Olympus, Center Valley, PA).

Quantification of vessel density

Frozen sections of wild type and knockout organs were acetone-fixed for 10 minutes and stained with antibody against the lymphatic marker, LYVE-1 [7], for 1 hour at 37°C, followed by incubation with DyLight 488-conjugated donkey anti-rabbit secondary antibodies for 1 hour at 37°C. To quantify LYVE-1 positive vessel density, 3–4 representative images per organ were acquired at 100X, 200X, or 400X magnifications for lungs, MFP, and liver, respectively, and the total number of positive vessels was enumerated and normalized per area of the field (mm^2). Lymphatic vessel density is presented as the

average number of LYVE-1 positive vessels per area of the field± SEM (n = 3–5 mice per group).

Measurement of mean vascular area

The mean vascular area of LYVE-1 positive staining per field was calculated as described previously [20], with slight modifications. Briefly, frozen sections were stained with rabbit anti-mLYVE-1 or goat anti-mVEGFR-3 primary antibodies and DyLight 549-conjugated donkey anti-rabbit or donkey anti-goat secondary antibodies, as described above. Fluorescent images were acquired at a constant exposure time at 200X and 400X magnifications for MFP and liver sections, respectively. Images were acquired on an Olympus BX41 upright microscope equipped with a DP70 digital camera and DP Controller software (Olympus, Center Valley, PA). Colored images were sequentially converted to 8-bit grayscale and then to a binary image using Image J software (http://rsbweb.nih.gov/ij/). The total area of LYVE-1 positive staining was then calculated using the analyze particles function of Image J that was set to measure the area of positive staining greater then 10 pixels in size to exclude any background staining. Mean vascular areas were calculated from 3 images per section ± SEM (n = 3–5 mice per group).

Measurement of mean fluorescent intensity

The mean fluorescent intensity (MFI) of VEGFR-3 and Prox1 positive staining was calculated as described previously [47], with slight modifications. Briefly, frozen sections were stained with goat anti-mVEGFR-3 or goat anti-Prox1 antibodies, followed by incubation with DyLight 549-conjugated donkey anti-goat secondary antibodies as described above. Fluorescent images were acquired at a constant exposure time at 400X magnification on an Olympus BX41 upright microscope equipped with a DP70 digital camera and DP Controller software (Olympus, Center Valley, PA). To exclude background staining, sections stained with secondary antibodies only were used to set the exposure time to below detectable level of background fluorescence. Digital RGB images acquired at a constant exposure time were converted to 8-bit grayscale. The fluorescent intensity for each pixel was calculated using the histogram function of Image J that was set up in the linear intensity range of 0 to 255 arbitrary units. Staining with secondary antibodies alone resulted in background fluorescence less than 10 units on this scale. MFI was calculated as the sum of the number of pixels above background multiplied by the intensity level in the range of 10–255 and divided by the total pixel number with intensity above 10 units. MFI values were obtained from 3 images per section (n = 3–5 mice per group) and presented as MFI units ± SEM. To compare the global reduction in fluorescent intensities in p50 KO and WT mice, representative RGB images were converted to 8-bit grayscale and visualized using the 3D interactive surface plot function of Image J.

Quantitative RT-PCR analysis

Four micrograms of total RNA extracted by Tri-reagent was reverse transcribed using a RevertAid First Strand cDNA synthesis kit, according to the manufacturer's protocol (Fermentas, Burlington, Ontario, Canada). Primers for qRT-PCR were designed against mouse and human CDS of angiogenic and lymphangiogenic proteins found in the NCBI database. Specific primer sequences were chosen using the Harvard primer database website (http://pga.mgh.harvard.edu/primerbank/index.html). All primers were purchased as annealed oligos from Integrated DNA Technologies (Coralville, IA) and sequences of primers used in this study are listed in Table 1. Quantitative RT-PCR was performed using Brilliant II SYBR Green Master Mix (Stratagene, La Jolla, CA) and an ABI 7500 Real-Time PCR machine (Applied BioSystems, Foster City, CA) according to the manufacturer's protocol. A typical qRT-PCR reaction consisted of an initial denaturation step at 95°C for 5 minutes followed by 40 cycles of denaturation at 95°C for 15 seconds and annealing,

extension, and reading at 60°C for 1 minute. A final melting curve for each primer was calculated by heating from 60 to 90°C. Data were normalized to β-actin and relative mRNA expression was determined using the ΔΔCt method as described previously [66].

Inflammatory cytokines and receptors qRT-PCR array

Two microgram of combined total MFP RNA from p50 KO and WT mice (n = 4 mice per group) was synthesized using a RevertAid First Strand cDNA synthesis kit, according to the manufacturer's protocol (Fermentas, Burlington, Ontario, Canada). Inflammatory gene expression was examined using a mouse inflammatory cytokines and receptors RT^2 Profiler PCR Array, according to the manufacturer's protocol (PAMM-011, SABiosciences, Fredrick, MD). Target gene expression was normalized to β-actin. Relative changes in mRNA expression of p50 KO MFP compared with WT was determined using the ΔΔCt method as described previously [66]. Data are presented as the β-actin normalized relative expression of transcripts in p50 KO MFP (n = 4 mice) compared with WT (n = 4 mice).

Statistical analysis

Statistical analysis was performed using SAS software (SAS Institute, Inc., Cary, NC). All results are expressed as the mean ± SEM and statistical differences were assessed by unpaired Student's *t*-test. Statistical significance was defined as $P<0.05$.

RESULTS

LYVE-1^+ vessel density is decreased in lung, liver and MFP of p50 KO mice

NF-κB dependent induction of inflammatory lymphangiogenesis has been shown in several animal models [5,26,38,41], including evidence obtained in our lab derived from a TG-induced peritonitis mouse model [20]. However, the specific role of the two major NF-κB proteins, p65 and p50, in normal LVD has not been yet examined. The role of p65 is exceedingly difficult to examine postnatally due to embryonic lethality of this genotype [68]. In contrast, p50 KO mice survive to adulthood [24] and present a useful *in vivo* model to clarify the impact of NF-κB p50 on density of lymphatic vessels that are required for the various functions of normal organs.

We previously showed that p50 is a direct transcriptional activator of the VEGFR-3 promoter in cultured LEC and that phosphorylation of p50 precedes both up-regulation of VEGFR-3 and the formation of new lymphatic vessels *in vivo* [20]. Based on these findings, we hypothesized that the absence of p50 may diminish the optimal density of lymphatic vessels in normal organs. To test this hypothesis, we determined LVD in six major normal organs (lung, liver, MFP, kidney, heart, and ovary) of adult female p50 KO and WT mice by enumerating LYVE-1^+ vessels. As previously reported [51], in addition to lymphatic vasculature, LYVE-1 was also detected in liver sinusoidal endothelium and thus both vascular types were enumerated. LYVE-1^+ lymphatic and sinusoidal vessel density was significantly decreased in three out of six organs of p50 KO mice as compared with WT. Table 2 shows the significant differences detected in: the lung (WT, 966 ± 90 vs. KO, 585 ± 55, $P < 0.001$); the liver (WT, 1307 ± 120 vs. KO, 1133 ± 83, $P = 0.05$); and the MFP (WT, 1917 ± 167 vs. KO, 1569 ± 144, $P < 0.001$). In contrast, kidney, heart, and ovary of p50 KO mice showed no significant changes compared with WT (Table 2). This suggested that NF-κB p50 might be important for achieving optimal LVD in the lung, liver, and MFP. However, p50 appears not to play a significant role in generating or maintaining LVD in kidney, heart and ovary.

Decreased LVD correlates with suppressed VEGFR-3 and Prox1 expression in the lungs of p50 KO mice

The most conspicuous decrease in LVD in p50 KO mice was in the lung tissues (~40%, Table 2). Because VEGFR-3 and Prox1 are central mediators of lymphangiogenesis [74,77] and their expression has been shown to be regulated by NF-κB p50 [20], we hypothesized that decreased pulmonary LVD might be mediated by deficient expression of VEGFR-3 or Prox1. To test this hypothesis, we compared mRNA levels of LYVE-1 with those of VEGFR-3 and Prox1. The results showed that expression levels of all three lymphatic markers (i.e., LYVE-1, VEGFR-3, and Prox1) were significantly reduced in the lungs of p50 KO mice compared with WT (Table 2). LYVE-1 transcripts were decreased by 32 ± 4% ($P = 0.03$), whereas VEGFR-3 and Prox1 were reduced by 25 ± 10% ($P = 0.17$) and 44 ± 4% ($P = 0.04$), respectively (Table 3). This finding suggests that NF-κB p50 regulates VEGFR-3 and Prox1 expression in lung lymphatic vessels that subsequently might result in reduced LVD in the lungs of p50 KO mice.

To determine whether the levels of VEGFR-3 and Prox1 proteins normalized per LYVE-1^+ lymphatic vessel area are also reduced (i.e., relative expression per lymphatic vessel), we calculated the relative MFI in individual lymphatic vessels (described in the Methods). The MFI values did not differ significantly between WT and KO suggesting that the observed reduction in VEGFR-3 and Prox1 expression levels (Table 3) is due to decreased density of positive vessels rather than to altered protein expression level in individual vessels. To clarify this point, we enumerated VEGFR-3^+ and Prox1^+ lymphatic vessels and normalized these values per tissue area. This analysis showed a significantly decreased density of VEGFR-3^+ and Prox1^+ lymphatic vessels by 30% ($P = 0.03$) and 20% ($P = 0.04$), respectively (Figure 1B, C). Moreover, when Prox1^+ nuclei were enumerated and normalized per LYVE-1^+ lymphatic vessel area, the decrease in Prox1^+ nuclei in the lymphatic vasculature of p50 KO mice reached 40% ($P = 0.01$) compared with p50 WT mice (Figure 1D). Collectively, these findings demonstrate that the absence of NF-κB p50 results in down-regulation of the expression of the key lymphangiogenic proteins, VEGFR-3 and Prox1, in adult pulmonary lymphatic vessels.

Decreased density of LYVE-1^+ vessels correlates with reduced expression of VEGFR-3 in the liver of p50 KO mice

LYVE-1^+ vessel density in the liver of p50 KO mice was also significantly reduced by 13.4% ($P = 0.05$) as compared with WT mice (Table 2). The reduction in LYVE-1^+ vessel density corresponded to a 44% decrease in LYVE-1 transcripts ($P = 0.02$) determined by qRT-PCR (data not shown). In line with decreased LYVE-1 transcripts, VEGFR-3 mRNA was also reduced by 29 ± 6% ($P = 0.004$, Table 3). The reduction in VEGFR-3 mRNA levels also corresponded to decreased expression of VEGFR-3 protein as determined by MFI analysis of slides double-stained with anti-VEGFR-3 and anti-LYVE-1 antibodies (Figure 2). These data indicate that the absence of p50 in the liver causes a coordinated decrease of LYVE-1^+ vessels and VEGFR-3 expressed on these vessels.

As previously reported, both lymphatic and blood hepatic sinusoidal endothelial cells express LYVE-1 and VEGFR-3 [51,78]. In p50 KO mice, VEGFR-3 protein significantly decreased by 51 ± 12% in both types of vascular cells compared with corresponding cells in WT mice ($P = 0.002$, Figure 2B and Table 3). Another perturbed vascular parameter in p50 KO livers was marked reduction in the total area of VEGFR-3^+ and LYVE-1^+ sinusoidal endothelium (Figure 2A). A similar phenotype has been demonstrated in *Tie2-Cre/IKKβ* mice with targeted disruption of canonical NF-κB p50 and p65 signaling in the endothelial cell compartment [33]. This report and our prior findings in cultured LECs suggested that NF-κB p50-mediated expression of VEGFR-3 might be important for the formation of the

LYVE-1-positive endothelium-lined hepatic sinusoids. To confirm this hypothesis, we quantified the mean vascular area of VEGFR-3^+/LYVE-1^+ vessels on images acquired from p50 KO and WT liver sections using Image J software. Compared with WT, the mean vascular area of VEGFR-3^+ and LYVE-1^+ vessels in p50 KO livers was significantly decreased by 40% and 55%, respectively (Figure 2C, D). Collectively, these findings suggest that decreased VEGFR-3 expression in p50 KO livers correlates with reduction of both blood and lymphatic vasculature in the livers of p50 KO mice, warranting future studies to interrogate the role of VEGFR-3 signaling in liver development.

Expression of Prox1 is decreased in both liver endothelial cells and hepatocytes of p50 KO mice

We previously reported that lymphatic expression of Prox1 is drastically increased in an inflammatory setting, presumably due to activation of the NF-κB pathway in the lymphatic endothelium [20]. However, the mechanisms regulating Prox1 expression under normal physiological conditions are presently unknown. Based on our prior findings [20], we postulated that NF-κB p50 might be required for regulation of Prox1 expression in normal adult organs. The liver is an interesting organ to test this hypothesis because in this tissue Prox1 is expressed in both lymphatic endothelial cells and hepatocytes [52]. We, therefore, analyzed livers from p50 KO and WT mice for Prox1 mRNA and protein by qRT-PCR and immunofluorescent staining, respectively (Figure 3). As compared with WT mice, expression of both Prox1 mRNA and protein were reduced by ~30% (Figure 3A, B and Table 3) with differences being statistically significant ($P = 0.03$). Reduction in Prox1 protein was observed in both hepatocytes and LYVE-1^+ endothelial cells (Figure 3B). Protein levels of Prox1 were also analyzed through comparison of MFI from Prox1-immunofluorescent staining of p50 KO and WT liver sections. This analysis also showed a highly significant ($P < 0.001$) decrease of 47 ± 3% in p50 KO liver cells as compared with WT counterparts (Figure 3C, D and Table 3). These findings indicate that in the context of liver tissue, NF-κB p50 has a significant impact on Prox1 expression in both endothelial and non-endothelial cell types.

Expression of Prox1 is decreased in the brain, but not in the heart, of p50 KO mice

In addition to hepatocytes, Prox1 has also been detected in several other non-lymphatic endothelial cell types including cardiomyocytes [62] and neurons [43]. We, therefore, sought to determine whether the absence of p50 in brains and hearts of p50 KO mice causes similar decrease in Prox1 expression as observed in the liver. To answer this question, Prox1 expression was analyzed on mRNA and protein levels using qRT-PCR and MFI, respectively. In the brain of p50 KO mice, transcripts and protein levels of Prox1 were reduced by 51 ± 12% and 25 ± 3%, respectively, compared with WT (Figure 4A–C and Table 3), with both values being statistically significant ($P = 0.01$, Table 3). In contrast, no change in Prox1 expression was observed in the heart of p50 KO (data not shown), suggesting that the regulatory effect of p50 NF-κB on Prox1 expression might be tissue-specific, being prominent in some organs but dispensable in others. This is consistent with similar tissue-dependent variable effects of deletion of p50 NF-κB that have been previously reported [67].

The MFPs of p50 KO mice exhibit decreased LYVE-1^+ LVD but aberrantly increased VEGFR-3 and Prox1 expression on lymphatic vasculature

The mouse mammary fat pad (MFP) is a tissue with very high LVD and expression of lymphatic-specific proteins. To analyze LVD in the MFP of KO and WT p50 mice, we compared the numbers of anti-LYVE-1 antibody stained structures in corresponding tissues (Figure 5A). This analysis revealed a ~20% decrease in density of LYVE-1^+ lymphatic vessels ($P < 0.001$, Table 2 and Figure 5B) and ~60% decrease in mean vascular area of

LYVE-1$^+$ staining per section area in p50 KO mice (P <0.001, Figure 5C). This finding was corroborated by qRT-PCR analysis that detected a corresponding 66 ± 9% decrease in LYVE-1 transcripts (P = 0.01, Figure 5D). Surprisingly, however, the number of VEGFR-3$^+$ and Prox1$^+$ lymphatic vessels was slightly higher in p50 KO mice compared with WT, although the differences did not reach statistical significance (data not shown). Additionally, the MFI of VEGFR-3 and Prox1 in lymphatic vessels was elevated by 134 ± 12% (P = 0.001) and 123 ± 15% (P = 0.05), respectively, in p50 KO mice compared with WT (Table 3). This was corroborated by statistically significant 1.8-fold and 2.4-fold increases in VEGFR-3 and Prox1 transcripts, respectively, as detected by qRT-PCR (Table 3). These findings indicated that although the density of LYVE-1$^+$ lymphatic vessels was reduced in the MFPs of p50 KO mice, the expression levels of VEGFR-3 and Prox1 per lymphatic vessel were significantly increased. These findings suggested that in the MFP context, p50 ablation reduced LVD despite overexpression of some lymphatic markers through possibly compensatory regulatory mechanisms.

Elevated VEGFR-3 and Prox1 expression on lymphatic vasculature of the MFPs of p50 KO mice is associated with altered profile of inflammatory mediators

To explain the paradoxical increase of VEGFR-3 and Prox1 in MFP lymphatic vessels, we hypothesized that the absence of p50 in this tissue is compensated by other members of the NF-κB family whose pro-inflammatory signaling up-regulates VEGFR-3 and Prox1 expression but is insufficient for generation of new lymphatic vessels. This is plausible because NF-κB subunits p65 and p52 have been previously reported to compensate for the lack of p50 [79]. To determine whether these subunits could be differentially expressed in tissues of p50 KO and WT mice, we analyzed p65 and p52 expression levels by qRT-PCR. This analysis revealed a nearly perfect correlation between changes in expression levels of VEGFR-3 and NF-κB p65 in each organ examined (Table 4). For example, both VEGFR-3 and p65 were reduced in lung and liver, elevated in MFP, and close to level of WT mice in kidney, heart, and brain. Similarly, the pattern of NF-κB p52 expression was highly correlative with Prox1 profile, with both genes being reduced in lung, liver and brain, elevated in MFP, and roughly unchanged in kidney and heart (Table 4). These data suggested that in the absence of p50 VEGFR-3 and Prox1 expression might be regulated by p65 and p52 NF-κB subunits overexpressed in the MFP of p50 KO mice.

Positive correlation between expression levels of VEGFR-3 and Prox1 and p65/p52 NF-κB subunits suggested that the MFP tissue compensates for the lack of p50 by up-regulating both canonical (p65) and non-canonical (p52) NF-κB pathways. This finding suggested that overexpression of p50-alternative transcription factors might create a pro-inflammatory rather than an anti-inflammatory environment. To test this hypothesis, we compared the expression levels of 84 NF-κB-dependent genes in the MFP of p50 KO and WT mice by using an inflammation gene-targeted PCR array. We found that a large portion of the tested genes (35 of 84, or 41.6% of total) expressed in the MFP of p50 KO mice were elevated by at least 1.5-fold compared with the MFP gene profile in WT mice (Table 5). A smaller fraction (28.5%) was down-regulated in p50 KO MFPs by at least 1.5-fold, while the level of remaining genes was unchanged. This finding suggested that VEGFR-3 and Prox1 are upregulated in MFPs of NF-κB p50 KO mice due to aberrant inflammation induced by compensatory over-expression of two factors of the NF-κB family, p65 and p52. However, the pathways induced by these two transcription factors were insufficient for reaching normal LVD mediated by p50 subunit as indicated by the 18% reduction in LVD in MFPs of p50 KO mice as compared with WT (Table 2). This evidence further underscores the essential role of the NF-κB p50 subunit in postnatal formation of lymphatic vessels in normal tissues.

DISCUSSION

Ablation of NF-κB p50 decreases lymphatic vessel density and lymphatic VEGFR-3 expression in some normal organs

We previously reported that the two most abundant NF-κB transcription factors, p50 and p65, are elevated prior to inflammatory lymphangiogenesis induced in a mouse peritonitis model *in vivo* [20]. We also showed in cultured LECs that p50, and to a lesser extent p65 protein, bind and activate the human VEGFR-3 promoter and induce its transcription [20]. Additionally, our data demonstrated that p50 but not the p65 subunit of NF-κB synergizes with Prox1, a lymphatic-expressed transcription factor, in up-regulating VEGFR-3 [20]. These data indicated a major role for NF-κB proteins, and in particular, NF-κB p50, in controlling the pro-lymphangiogenic intracellular milieu necessary for creating and maintaining the lymphatic vasculature. Other groups have demonstrated that NF-κB proteins, and particularly p50 subunit, are constitutively expressed in normal adult lymphatic endothelium [64] and contribute to normal function of lymphatic vessels in adults [37].

Based on these prior data and reports, we hypothesized that mice lacking the NF-κB p50 subunit might have lower expression of Prox1 and VEGFR-3 that subsequently would result in reduced LVD in normal organs. Tissue analysis from p50 KO mice confirmed that indeed three out of six organs with lymphatic networks (e.g., lung, liver, and MFP) exhibited decreased LYVE-1^+ vessel density (Figures 1, 2 and Table 2). Moreover, reduction of LVD in most affected organs corresponded to significant suppression of VEGFR-3 and Prox1 expression (Tables 2 and 3) suggesting that these genes are constitutively regulated by p50 on a transcriptional level. This is in line with other studies reporting that constitutive activity of NF-κB p50 is essential for maintaining various immune functions under normal conditions [10, 11, 19, 54]. This conclusion is also consistent with our prior findings demonstrating that silencing NF-κB expression significantly reduced levels of Prox1 and VEGFR-3 in untreated cultured LEC [20], therefore suggesting that p50 is important for normal LEC functions. Two independent publications support this conclusion by demonstrating constitutive activity of the promoter of p105 (a p50 precursor) in the LEC of transgenic *κB-lacZ* mice that underwent further up-regulation upon exposure to inflammatory factors [37, 64]. Collectively, these data suggest that NF-κB p50 regulates expression of VEGFR-3 and Prox1 in LEC under both normal and inflamed conditions, and that the level of these proteins is important for normal lymphatic vessel development in some organs.

In contrast to the lung, liver, and MFP, several other organs (e.g., kidney, heart, and ovary) of NF-κB p50 KO mice showed no significant changes in LVD or VEGFR-3 and Prox1 expression (Tables 2 and 3). In these unaffected p50 KO organs, expression of NF-κB p65 remained close to or equal to the normal levels in WT mice (Table 5), suggesting that signaling through p65 homodimers or p65/p52 heterodimers might compensate for the lack of p50 in an organ-specific manner (summarized in Figure 6). The maintenance of the inflammatory milieu by p65 in the absence of p50 has been previously shown in inflamed hearts and kidneys of p50 KO mice [57,70]. Inflammatory stimuli that activate NF-κB p65 homodimers (e.g., LPS and TNF-α) are also known to induce lymphangiogenesis [6,37], suggesting that under some circumstances NF-κB p65 homodimers are sufficient to regulate both inflammation-induced lymphangiogenesis and normal lymphatic vessel development. Due to the embryonic lethality of p65 KO mice [8], it is currently not possible to determine whether NF-κB p65 is essential for postnatal lymphangiogenesis under normal conditions. However, lack of differences in LVD in aforementioned organs strongly suggests that p65 and the non-canonical NF-κB subunits might compensate for the absent function of p50 protein.

Tissue-specific regulation of VEGFR-3 and Prox1 expression might also be mediated by differential expression of NF-κB p50 binding partners, such as NF-κB p65, that are required for activating gene transcription, because NF-κB p50 lacks a consensus transactivation domain [9]. Moreover, relative expression of NF-κB p50 and p65 subunits under different conditions and cellular contexts likely modulates the ratio of p50/p65 heterodimers and p50/p50 or p65/p65 homodimers. This may have significant impact on gene regulation because all NF-κB dimers are able to bind to the same κB response element [13,30], albeit with variable affinity [13,30] and functional consequences (i.e., promoter activation or repression) [13,30]. Presence or absence of other transcription factors and regulatory proteins outside the NF-κB family may also modulate NF-κB p50 function. NF-κB p50/p50 homodimers interact with the transcriptional co-activators, such as Bcl-3 [42] or C/EBP proteins [14], that determine whether p50/p50 functions as a transcriptional activator (e.g., Bcl-2 [42] and PDGF-A promoters [2]) or repressor (e.g., TNF-α and IL-8 promoters [72]). We recently have shown that co-expression of Prox1 with NF-κB p50 synergistically activated the VEGFR-3 promoter [20], suggesting that Prox1 might be a lymphatic-specific co-activator of p50. This may be possible through recruitment of the common binding partner and transcriptional co-activator, CBP/p300 [16]. Moreover, synergy between NF-κB p50 and Prox1 and evidence that NF-κB p50 may regulate Prox1 expression (Table 2, and Figures 1 and 3), suggests that Prox1 may affect the function of NF-κB p50 in two ways: by amplifying p50 signaling and by imparting lymphatic specificity to the activated NF-κB pathway.

Ablation of NF-κB p50 in the MFP creates abnormal environment characterized by reduced LVD but elevated VEGFR-3 and Prox1

The lymphatics in the MFP of p50 KO mice were uniquely affected by the absence of NF-κB p50: similarly to lungs and liver, LYVE-1^+ vessel density was significantly reduced (Figure 5 and Table 2), however, the expression of VEGFR-3 and Prox1 was paradoxically elevated (Table 3). We drew two conclusions from these observations: 1) up-regulation of Prox1 and VEGFR-3 suggests compensatory overexpression of p50-alternative NF-κB factors; and 2) normal MFP lymphatic vessel development might require p50-specific signals other than Prox1 and VEGFR-3. Both of these conclusions are supported by data presented here and are plausible based on the findings of previous reports. Tables 4 and 5 show that, in contrast to other organs, the MFP of p50 in KO mice is characterized by significantly increased expression of NF-κB p65 and p52 subunits as well as a greater than 150% increase in expression levels of 35 inflammatory cytokines. These findings are consistent with a previous report demonstrating that p52 NF-κB might compensate for the lack of p50 signaling in TNF-α treated mammary epithelial cells [79]. Additionally, NF-κB dimers that do not include the p50 subunit (e.g., p65/p65 and p65/p52) are known to bind and activate κB response elements [65], suggesting that in the absence of p50 these dimers could independently activate the VEGFR-3 and Prox1 promoters. This is also supported by our recent finding that p65 binds and activates the VEGFR-3 promoter [20], albeit with much lower efficiency than the p50 subunit. Collectively, these data indicate that increased expression of p65 and p52 in p50 KO MFP compensates for the lack of p50 by increasing the expression of VEGFR-3 and Prox1 (summarized in Figure 6). However, the increased levels of these pro-lymphangiogenic factors was insufficient to fully compensate for optimal lymphatic vessel development observed in the MFP of WT mice.

The later conclusion implies that normal MFP lymphangiogenesis requires some p50-specific factors in addition to VEGFR-3 and Prox1. Table 5 shows that approximately 15 of NF-κB p50-dependent inflammatory cytokines, including IL-3, lymphotoxin α, and lymphotoxin β, are down-regulated by more than 2-fold in MFPs of p50 KO mice. This is in line with previous findings demonstrating that lymphotoxins α and β as well as IL-3 are

direct activators of LEC and lymphangiogenesis *in vivo* [20,21,25,44,49,58]. Taken together, the data presented here suggest that p50-dependent IL-3 and lymphotoxin pathways might be important for maintaining normal MFP lymphatic vessel density.

Regulation of lymphatic-specific VEGFR-3 and Prox1 expression by NF-κB p50 *in vivo*

Although Prox1 has been shown to regulate VEGFR-3 in cultured endothelial cells [20,32,48,56,59], very few studies correlated Prox1 expression in relation to VEGFR-3 *in vivo*. We have previously shown that Prox1 binds and activates the VEGFR-3 promoter [20], suggesting that Prox1 is a direct transcriptional regulator of the VEGFR-3 gene. This is consistent with novel findings presented here that demonstrate complete overlap between expression patterns of Prox1 and VEGFR-3 in normal organs of p50 KO as compared with WT mice (Table 3). These data support the notion that one of the functions of Prox1 in adult LEC is to control levels of VEGFR-3 expression that are required for robust lymphangiogenic response.

The other important and currently open question in this context is the identity of factors that control Prox1 expression, particularly those that elevate its expression in LEC and suppress it in most non-lymphatic cell types. We previously reported that NF-κB-dependent inflammation induced lymphatic-specific Prox1 expression, which preceded inflammatory lymphangiogenesis *in vivo* [20]. Additionally, using *in vitro* techniques, we also demonstrated that manipulating NF-κB p50 signaling correlated with Prox1 expression in LEC [20]. Similar results have been obtained in several independent studies showing that Prox1 is increased in endothelial cells treated with IL-3 [25] or another potent activator of the NF-κB pathway, Kaposi Sarcoma Herpes Virus [31]. The notion that Prox1 might be regulated by NF-κB p50 is also supported by the evidence from this study demonstrating decreased expression of Prox1 in the liver, lungs, and brain of p50 KO mice (Table 3). However, other organs were not affected suggesting the existence of additional tissue-specific factors controlling Prox1 expression. This tissue-dependent variability in Prox1 expression and corresponding defects in lymphatic vasculature is similar to findings in *Fiaf* −/− mice that have reduced Prox1 expression and lymphatic vascular defects in the small intestine, but normal level of Prox1 and unaffected lymphatic vasculature in all other organs [4]. The tissue-specific regulation of Prox1 expression may also account for the parallel normal levels of VEGFR-3 expression in some organs tested here, further supporting our previous observations that Prox1 may activate the VEGFR-3 promoter in both p50-dependent and independent manners [20].

NF-κB p50 also regulates Prox1 in some non-lymphatic cell types

Although Prox1 is considered a lymphatic-specific marker [36], its expression has also been reported in various non-lymphatic tissues including liver [69], brain [43], heart [62], pancreas [75], eye [18,71], ear [17], and small intestine [60]. In line with these observations, we detected Prox1 in non-lymphatic endothelial cells in several normal organs of p50 KO and WT mice, including liver hepatocytes, brain neurons, and heart cardiomyocytes. Although no changes in Prox1 expression were detected in cardiomyocytes, this protein was significantly downregulated in both hepatocytes and neurons of p50 KO mice compared with WT (Figures 3, 4 and Table 3). This indicates that NF-κB p50 regulates Prox1 not only in lymphatic endothelium but also in some non-lymphatic cell types.

Prox1 was reported to play an essential role in liver morphogenesis [69], hepatocyte migration [69], and liver metabolism [12]. No changes, however, were previously noted in the liver function of NF-κB p50 KO mice [39], suggesting that the remaining ~50% of Prox1 protein (Figure 3D) is sufficient for normal hepatogenesis. In contrast, genetic ablation of p50 was reported to impair hippocampal neurogenesis [34] and to increase age-

related neural degeneration [45]. The molecular mechanisms underlying these disorders in p50 KO mice are currently unclear. Our discovery that Prox1 expression in non-lymphatic tissues (e.g., brain) is potentially regulated by NF-κB p50 might open new avenues in understanding of the function of Prox1 in adult tissues under normal, inflamed and pathological circumstances. Future validation of NF-κB mediated control of Prox1 expression is warranted because of the significance of Prox1 function in both lymphatic endothelium and other cell types.

CONCLUSIONS

This work was initially inspired by the impact of the NF-κB p50 subunit on transactivation of VEGFR-3 promoter [20] and subsequently evolved to a systematic comparison of VEGFR-3 and Prox1 expression in the lymphatics of normal organs in p50 KO and WT mice. During this analysis, we have made several novel observations such as: 1) original evidence for the role of NF-κB p50 in organ-specific maintenance of lymphatic vessel density and expression of the key pro-lymphangiogenic proteins, VEGFR-3 and Prox1, under normal conditions; 2) strong associations among VEGFR-3, Prox1 and lymphatic vessel density that are consistent with the notion that NF-κB regulates Prox1 and VEGFR-3 expression *in vivo*; and 3) novel evidence demonstrating the suppression of Prox1 expression in p50 KO hepatocytes and neurons, suggesting for the first time that NF-κB p50 regulates Prox1 expression in non-lymphatic cell types. Although these data support the idea that NF-κB p50 is involved in regulation of VEGFR-3 and Prox1 expression, transcription of these genes might be additionally controlled by p65 and p52 as well as by other regulatory factors outside of the NF-κB family. Nevertheless, our observations are important for documenting lymphatic vessel density and expression levels of major lymphangiogenic factors in adult normal organs while highlighting the possible roles of the NF-κB p50 subunit in normal physiology of both endothelial and non-endothelial tissues.

Acknowledgments

Support: This study was funded, in part, by the National Institute of Health (#1R15CA125682-01 and #1R01CA140732-01A1 to SR), Illinois William E. McElroy Foundation (SR) and SIUSOM Excellence in Medicine awards (SR), and by a Department of Defense Breast Cancer Research Program pre-doctoral traineeship (#BC073318 to MJF).

The authors thank Dr. Linda Toth for providing p50 WT and KO mice used in the initial experiments. We also gratefully thank Heather McKinnon, Kathleen Brancato, and Shelly Reeter for their assistance in tissue sectioning and immunostaining. This work was supported by grants from the National Institute of Health (#1R15CA125682-01 and #1R01CA140732-01A1), Illinois William E. McElroy Foundation, and SIUSOM Excellence in Medicine awards (SR), and a Department of Defense Breast Cancer Research Program pre-doctoral traineeship (#BC073318 to MJF).

References

1. Ahn KS, Aggarwal BB. Transcription factor NF-kappaB: a sensor for smoke and stress signals. Ann N Y Acad Sci. 2005; 1056:218–33. [PubMed: 16387690]
2. Aizawa K, Suzuki T, Kada N, Ishihara A, Kawai-Kowase K, et al. Regulation of platelet-derived growth factor-A chain by Kruppel-like factor 5: new pathway of cooperative activation with nuclear factor-kappaB. J Biol Chem. 2004; 279:70–6. [PubMed: 14573617]
3. Alitalo K, Tammela T, Petrova TV. Lymphangiogenesis in development and human disease. Nature. 2005; 438:946–53. [PubMed: 16355212]
4. Backhed F, Crawford PA, O'Donnell D, Gordon JI. Postnatal lymphatic partitioning from the blood vasculature in the small intestine requires fasting-induced adipose factor. Proc Natl Acad Sci U S A. 2007; 104:606–11. [PubMed: 17202268]

5. Baluk P, Tammela T, Ator E, Lyubynska N, Achen MG, et al. Pathogenesis of persistent lymphatic vessel hyperplasia in chronic airway inflammation. J Clin Invest. 2005; 115:247–57. [PubMed: 15668734]
6. Baluk P, Yao LC, Feng J, Romano T, Jung SS, et al. TNF-alpha drives remodeling of blood vessels and lymphatics in sustained airway inflammation in mice. J Clin Invest. 2009; 119:2954–64. [PubMed: 19759514]
7. Banerji S, Ni J, Wang SX, Clasper S, Su J, et al. LYVE-1, a new homologue of the CD44 glycoprotein, is a lymph-specific receptor for hyaluronan. J Cell Biol. 1999; 144:789–801. [PubMed: 10037799]
8. Beg AA, Sha WC, Bronson RT, Ghosh S, Baltimore D. Embryonic lethality and liver degeneration in mice lacking the RelA component of NF-kappa B. Nature. 1995; 376:167–70. [PubMed: 7603567]
9. Beinke S, Ley SC. Functions of NF-kappaB1 and NF-kappaB2 in immune cell biology. Biochem J. 2004; 382:393–409. [PubMed: 15214841]
10. Cariappa A, Liou HC, Horwitz BH, Pillai S. Nuclear factor kappa B is required for the development of marginal zone B lymphocytes. J Exp Med. 2000; 192:1175–82. [PubMed: 11034607]
11. Chang M, Lee AJ, Fitzpatrick L, Zhang M, Sun SC. NF-kappa B1 p105 regulates T cell homeostasis and prevents chronic inflammation. J Immunol. 2009; 182:3131–8. [PubMed: 19234210]
12. Charest-Marcotte A, Dufour CR, Wilson BJ, Tremblay AM, Eichner LJ, et al. The homeobox protein Prox1 is a negative modulator of ERR{alpha}/PGC-1{alpha} bioenergetic functions. Genes Dev. 2010; 24:537–42. [PubMed: 20194433]
13. Chen FE, Ghosh G. Regulation of DNA binding by Rel/NF-kappaB transcription factors: structural views. Oncogene. 1999; 18:6845–52. [PubMed: 10602460]
14. Chen Q, Dowhan DH, Liang D, Moore DD, Overbeek PA. CREB-binding protein/p300 co-activation of crystallin gene expression. J Biol Chem. 2002; 277:24081–9. [PubMed: 11943779]
15. Colotta F, Allavena P, Sica A, Garlanda C, Mantovani A. Cancer-related inflammation, the seventh hallmark of cancer: links to genetic instability. Carcinogenesis. 2009; 30:1073–81. [PubMed: 19468060]
16. Cui W, Tomarev SI, Piatigorsky J, Chepelinsky AB, Duncan MK. Mafs, Prox1, and Pax6 can regulate chicken betaB1-crystallin gene expression. J Biol Chem. 2004; 279:11088–95. [PubMed: 14707122]
17. Dabdoub A, Puligilla C, Jones JM, Fritzsch B, Cheah KS, et al. Sox2 signaling in prosensory domain specification and subsequent hair cell differentiation in the developing cochlea. Proc Natl Acad Sci U S A. 2008; 105:18396–401. [PubMed: 19011097]
18. Dyer MA, Livesey FJ, Cepko CL, Oliver G. Prox1 function controls progenitor cell proliferation and horizontal cell genesis in the mammalian retina. Nat Genet. 2003; 34:53–8. [PubMed: 12692551]
19. Ferguson AR, Corley RB. Accumulation of marginal zone B cells and accelerated loss of follicular dendritic cells in NF-kappaB p50-deficient mice. BMC Immunol. 2005; 6:8. [PubMed: 15836790]
20. Flister MJ, Wilber A, Hall KL, Iwata C, Miyazono K, et al. Inflammation induces lymphangiogenesis through up-regulation of VEGFR-3 mediated by NF-kappaB and Prox1. Blood. 2010; 115:418–29. [PubMed: 19901262]
21. Furtado GC, Marinkovic T, Martin AP, Garin A, Hoch B, et al. Lymphotoxin beta receptor signaling is required for inflammatory lymphangiogenesis in the thyroid. Proc Natl Acad Sci U S A. 2007; 104:5026–31. [PubMed: 17360402]
22. Ganta VC, Cromer W, Mills GL, Traylor J, Jennings M, et al. Angiopoietin-2 in experimental colitis. Inflamm Bowel Dis. 2010; 16:1029–39. [PubMed: 19902545]
23. Gilmore TD. Introduction to NF-kappaB: players, pathways, perspectives. Oncogene. 2006; 25:6680–4. [PubMed: 17072321]
24. Gotaskie GE, Andreassi BF. Paclitaxel: a new antimitotic chemotherapeutic agent. Cancer Pract. 1994; 2:27–33. [PubMed: 7914453]

25. Groger M, Loewe R, Holnthoner W, Embacher R, Pillinger M, et al. IL-3 induces expression of lymphatic markers Prox-1 and podoplanin in human endothelial cells. J Immunol. 2004; 173:7161–9. [PubMed: 15585837]
26. Guo R, Zhou Q, Proulx ST, Wood R, Ji RC, et al. Inhibition of lymphangiogenesis and lymphatic drainage via vascular endothelial growth factor receptor 3 blockade increases the severity of inflammation in a mouse model of chronic inflammatory arthritis. Arthritis Rheum. 2009; 60:2666–76. [PubMed: 19714652]
27. Henno A, Blacher S, Lambert C, Colige A, Seidel L, et al. Altered expression of angiogenesis and lymphangiogenesis markers in the uninvolved skin of plaque-type psoriasis. Br J Dermatol. 2009; 160:581–90. [PubMed: 18945297]
28. Hirakawa S, Brown LF, Kodama S, Paavonen K, Alitalo K, Detmar M. VEGF-C-induced lymphangiogenesis in sentinel lymph nodes promotes tumor metastasis to distant sites. Blood. 2007; 109:1010–7. [PubMed: 17032920]
29. Hoffmann A, Baltimore D. Circuitry of nuclear factor kappaB signaling. Immunol Rev. 2006; 210:171–86. [PubMed: 16623771]
30. Hoffmann A, Natoli G, Ghosh G. Transcriptional regulation via the NF-kappaB signaling module. Oncogene. 2006; 25:6706–16. [PubMed: 17072323]
31. Hong YK, Foreman K, Shin JW, Hirakawa S, Curry CL, et al. Lymphatic reprogramming of blood vascular endothelium by Kaposi sarcoma-associated herpesvirus. Nat Genet. 2004; 36:683–5. [PubMed: 15220917]
32. Hong YK, Harvey N, Noh YH, Schacht V, Hirakawa S, et al. Prox1 is a master control gene in the program specifying lymphatic endothelial cell fate. Dev Dyn. 2002; 225:351–7. [PubMed: 12412020]
33. Hou Y, Li F, Karin M, Ostrowski MC. Analysis of the IKKbeta/NF-kappaB signaling pathway during embryonic angiogenesis. Dev Dyn. 2008; 237:2926–35. [PubMed: 18816823]
34. Denis-Donini S, Dellarole A, Crociara P, Francese MT, Bortolotto V, et al. Impaired adult neurogenesis associated with short-term memory defects in NF-kappaB p50-deficient mice. J Neurosci. 2008; 28:3911–9. [PubMed: 18400889]
35. Johnson LA, Jackson DG. Cell traffic and the lymphatic endothelium. Ann N Y Acad Sci. 2008; 1131:119–33. [PubMed: 18519965]
36. Johnson NC, Dillard ME, Baluk P, McDonald DM, Harvey NL, et al. Lymphatic endothelial cell identity is reversible and its maintenance requires Prox1 activity. Genes Dev. 2008; 22:3282–91. [PubMed: 19056883]
37. Kang S, Lee SP, Kim KE, Kim HZ, Memet S, Koh GY. Toll-like receptor 4 in lymphatic endothelial cells contributes to LPS-induced lymphangiogenesis by chemotactic recruitment of macrophages. Blood. 2009; 113:2605–13. [PubMed: 19098273]
38. Kataru RP, Jung K, Jang C, Yang H, Schwendener RA, et al. Critical role of CD11b+ macrophages and VEGF in inflammatory lymphangiogenesis, antigen clearance, and inflammation resolution. Blood. 2009; 113:5650–9. [PubMed: 19346498]
39. Kato A, Edwards MJ, Lentsch AB. Gene deletion of NF-kappa B p50 does not alter the hepatic inflammatory response to ischemia/reperfusion. J Hepatol. 2002; 37:48–55. [PubMed: 12076861]
40. Kerjaschki D, Huttary N, Raab I, Regele H, Bojarski-Nagy K, et al. Lymphatic endothelial progenitor cells contribute to de novo lymphangiogenesis in human renal transplants. Nat Med. 2006; 12:230–4. [PubMed: 16415878]
41. Kunstfeld R, Hirakawa S, Hong YK, Schacht V, Lange-Asschenfeldt B, et al. Induction of cutaneous delayed-type hypersensitivity reactions in VEGF-A transgenic mice results in chronic skin inflammation associated with persistent lymphatic hyperplasia. Blood. 2004; 104:1048–57. [PubMed: 15100155]
42. Kurland JF, Kodym R, Story MD, Spurgers KB, McDonnell TJ, Meyn RE. NF-kappaB1 (p50) homodimers contribute to transcription of the bcl-2 oncogene. J Biol Chem. 2001; 276:45380–6. [PubMed: 11567031]
43. Lavado A, Oliver G. Prox1 expression patterns in the developing and adult murine brain. Dev Dyn. 2007; 236:518–24. [PubMed: 17117441]

44. Lo JC, Basak S, James ES, Quiambo RS, Kinsella MC, et al. Coordination between NF-kappaB family members p50 and p52 is essential for mediating LTbetaR signals in the development and organization of secondary lymphoid tissues. Blood. 2006; 107:1048–55. [PubMed: 16195333]
45. Lu ZY, Yu SP, Wei JF, Wei L. Age-related neural degeneration in nuclear-factor kappaB p50 knockout mice. Neuroscience. 2006; 139:965–78. [PubMed: 16533569]
46. Makinen T, Veikkola T, Mustjoki S, Karpanen T, Catimel B, et al. Isolated lymphatic endothelial cells transduce growth, survival and migratory signals via the VEGF-C/D receptor VEGFR-3. EMBO J. 2001; 20:4762–73. [PubMed: 11532940]
47. Mancuso MR, Davis R, Norberg SM, O'Brien S, Sennino B, et al. Rapid vascular regrowth in tumors after reversal of VEGF inhibition. J Clin Invest. 2006; 116:2610–21. [PubMed: 17016557]
48. Mishima K, Watabe T, Saito A, Yoshimatsu Y, Imaizumi N, et al. Prox1 induces lymphatic endothelial differentiation via integrin alpha9 and other signaling cascades. Mol Biol Cell. 2007; 18:1421–9. [PubMed: 17287396]
49. Mounzer RH, Svendsen OS, Baluk P, Bergman CM, Padera TP, et al. Lymphotoxin alpha contributes to lymphangiogenesis. Blood. 2010
50. Mouta C, Heroult M. Inflammatory triggers of lymphangiogenesis. Lymphat Res Biol. 2003; 1:201–18. [PubMed: 15624438]
51. Mouta CC, Nasser SM, di Tomaso E, Padera TP, Boucher Y, et al. LYVE-1 is not restricted to the lymph vessels: expression in normal liver blood sinusoids and down-regulation in human liver cancer and cirrhosis. Cancer Res. 2001; 61:8079–84. [PubMed: 11719431]
52. Oliver G, Sosa-Pineda B, Geisendorf S, Spana EP, Doe CQ, Gruss P. Prox 1, a prospero-related homeobox gene expressed during mouse development. Mech Dev. 1993; 44:3–16. [PubMed: 7908825]
53. Olszewski WL. The lymphatic system in body homeostasis: physiological conditions. Lymphat Res Biol. 2003; 1:11–21. [PubMed: 15624317]
54. Ouaaz F, Arron J, Zheng Y, Choi Y, Beg AA. Dendritic cell development and survival require distinct NF-kappaB subunits. Immunity. 2002; 16:257–70. [PubMed: 11869686]
55. Paavonen K, Puolakkainen P, Jussila L, Jahkola T, Alitalo K. Vascular endothelial growth factor receptor-3 in lymphangiogenesis in wound healing. Am J Pathol. 2000; 156:1499–504. [PubMed: 10793061]
56. Pan MR, Chang TM, Chang HC, Su JL, Wang HW, Hung WC. Sumoylation of Prox1 controls its ability to induce VEGFR3 expression and lymphatic phenotypes in endothelial cells. J Cell Sci. 2009; 122:3358–64. [PubMed: 19706680]
57. Panzer U, Steinmetz OM, Turner JE, Meyer-Schwesinger C, von RC, et al. Resolution of renal inflammation: a new role for NF-kappaB1 (p50) in inflammatory kidney diseases. Am J Physiol Renal Physiol. 2009; 297:F429–F439. [PubMed: 19458123]
58. Paz-Priel I, Cai DH, Wang D, Kowalski J, Blackford A, et al. CCAAT/enhancer binding protein alpha (C/EBPalpha) and C/EBPalpha myeloid oncoproteins induce bcl-2 via interaction of their basic regions with nuclear factor-kappaB p50. Mol Cancer Res. 2005; 3:585–96. [PubMed: 16254192]
59. Petrova TV, Makinen T, Makela TP, Saarela J, Virtanen I, et al. Lymphatic endothelial reprogramming of vascular endothelial cells by the Prox-1 homeobox transcription factor. EMBO J. 2002; 21:4593–9. [PubMed: 12198161]
60. Petrova TV, Nykanen A, Norrmen C, Ivanov KI, Andersson LC, et al. Transcription factor PROX1 induces colon cancer progression by promoting the transition from benign to highly dysplastic phenotype. Cancer Cell. 2008; 13:407–19. [PubMed: 18455124]
61. Ran S, Volk L, Hall K, Flister MJ. Lymphangiogenesis and lymphatic metastasis in breast cancer. Pathophysiology. 2010; 17:229–51. [PubMed: 20036110]
62. Risebro CA, Searles RG, Melville AA, Ehler E, Jina N, et al. Prox1 maintains muscle structure and growth in the developing heart. Development. 2009; 136:495–505. [PubMed: 19091769]
63. Roberts N, Kloos B, Cassella M, Podgrabinska S, Persaud K, et al. Inhibition of VEGFR-3 activation with the antagonistic antibody more potently suppresses lymph node and distant metastases than inactivation of VEGFR-2. Cancer Res. 2006; 66:2650–7. [PubMed: 16510584]

64. Saban MR, Memet S, Jackson DG, Ash J, Roig AA, et al. Visualization of lymphatic vessels through NF-kappaB activity. Blood. 2004; 104:3228–30. [PubMed: 15271802]
65. Saccani S, Pantano S, Natoli G. Modulation of NF-kappaB activity by exchange of dimers. Mol Cell. 2003; 11:1563–74. [PubMed: 12820969]
66. Schmittgen TD, Livak KJ. Analyzing real-time PCR data by the comparative C(T) method. Nat Protoc. 2008; 3:1101–8. [PubMed: 18546601]
67. Sha WC, Liou HC, Tuomanen EI, Baltimore D. Targeted disruption of the p50 subunit of NF-kappa B leads to multifocal defects in immune responses. Cell. 1995; 80:321–30. [PubMed: 7834752]
68. Sledge GW Jr, Miller KD. Metastatic breast cancer: the role of chemotherapy. Semin Oncol. 1999; 26:6–10. [PubMed: 10190779]
69. Sosa-Pineda B, Wigle JT, Oliver G. Hepatocyte migration during liver development requires Prox1. Nat Genet. 2000; 25:254–5. [PubMed: 10888866]
70. Timmers L, van Keulen JK, Hoefer IE, Meijs MF, van MB, et al. Targeted deletion of nuclear factor kappaB p50 enhances cardiac remodeling and dysfunction following myocardial infarction. Circ Res. 2009; 104:699–706. [PubMed: 19168865]
71. Tomarev SI, Sundin O, Banerjee-Basu S, Duncan MK, Yang JM, Piatigorsky J. Chicken homeobox gene Prox 1 related to Drosophila prospero is expressed in the developing lens and retina. Dev Dyn. 1996; 206:354–67. [PubMed: 8853985]
72. Tong X, Yin L, Washington R, Rosenberg DW, Giardina C. The p50-p50 NF-kappaB complex as a stimulus-specific repressor of gene activation. Mol Cell Biochem. 2004; 265:171–83. [PubMed: 15543947]
73. Vallabhapurapu S, Karin M. Regulation and function of NF-kappaB transcription factors in the immune system. Annu Rev Immunol. 2009; 27:693–733. [PubMed: 19302050]
74. Veikkola T, Jussila L, Makinen T, Karpanen T, Jeltsch M, et al. Signalling via vascular endothelial growth factor receptor-3 is sufficient for lymphangiogenesis in transgenic mice. EMBO J. 2001; 20:1223–31. [PubMed: 11250889]
75. Wang J, Kilic G, Aydin M, Burke Z, Oliver G, Sosa-Pineda B. Prox1 activity controls pancreas morphogenesis and participates in the production of “secondary transition” pancreatic endocrine cells. Dev Biol. 2005; 286:182–94. [PubMed: 16122728]
76. Wigle JT, Harvey N, Detmar M, Lagutina I, Grosveld G, et al. An essential role for Prox1 in the induction of the lymphatic endothelial cell phenotype. EMBO J. 2002; 21:1505–13. [PubMed: 11927535]
77. Wigle JT, Oliver G. Prox1 function is required for the development of the murine lymphatic system. Cell. 1999; 98:769–78. [PubMed: 10499794]
78. Witmer AN, Dai J, Weich HA, Vrensen GF, Schlingemann RO. Expression of vascular endothelial growth factor receptors 1, 2, and 3 in quiescent endothelia. J Histochem Cytochem. 2002; 50:767–77. [PubMed: 12019293]
79. Zhang J, Warren MA, Shoemaker SF, Ip MM. NFkappaB1/p50 is not required for tumor necrosis factor-stimulated growth of primary mammary epithelial cells: implications for NFkappaB2/p52 and RelB. Endocrinology. 2007; 148:268–78. [PubMed: 17008396]
80. Zhang Q, Lu Y, Proulx ST, Guo R, Yao Z, et al. Increased lymphangiogenesis in joints of mice with inflammatory arthritis. Arthritis Res Ther. 2007; 9:R118. [PubMed: 17997858]
81. Zumsteg A, Christofori G. Corrupt policemen: inflammatory cells promote tumor angiogenesis. Curr Opin Oncol. 2009; 21:60–70. [PubMed: 19125020]

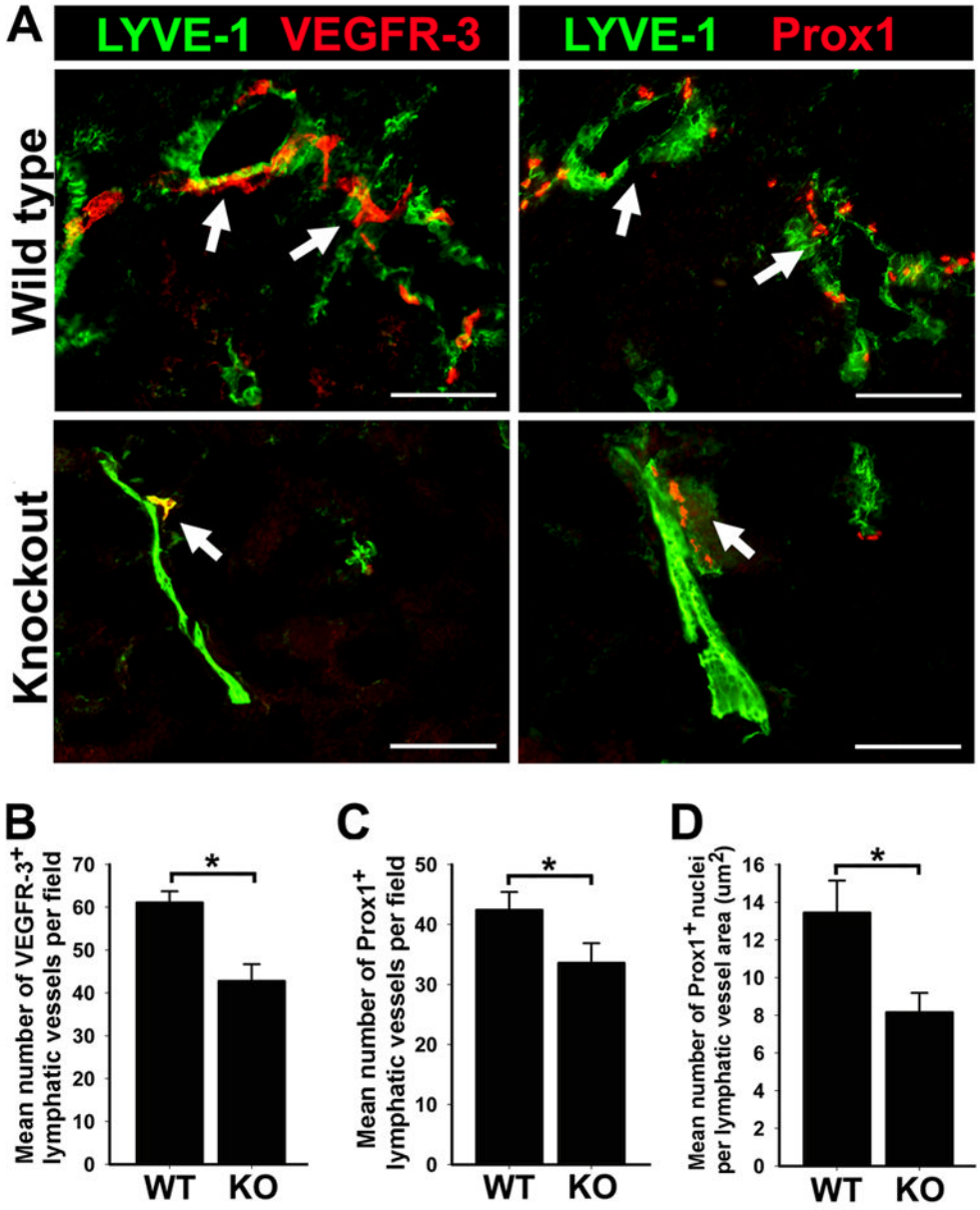

Figure 1.

Decreased lymphatic vessel density and reduced expression of Prox1 and VEGFR-3 in the lungs of p50 KO mice compared with WT. (**A**) Double immunofluorescent staining with anti-LYVE-1 and anti-VEGFR-3 or anti-Prox1 antibodies in serial sections of p50 KO and WT lungs, showing reduced lymphatic vessel density. Arrows indicate overlapping expression of VEGFR-3 and Prox1 on LYVE-1$^+$ lymphatic vessels on serial sections of p50 KO and WT lungs. Scale bar represents 100 μm. Mean lymphatic vessel density of VEGFR-3 (**B**) and Prox1 (**C**) positive vessels was measured from 3 images of p50 KO and WT lungs (n = 5 mice per group) acquired at 200X magnification. Data are presented as the mean vascular area ± SEM. The *P* values represent *<0.05 and **<0.01 as determined by Student's unpaired t-test. (**D**) The number of Prox1 positive nuclei were enumerated in 5 images of p50 KO and WT lungs (n = 3–4 mice per group) acquired at 200X magnification. Density of Prox1 positive nuclei was normalized per LYVE-1 positive lymphatic vessel area

(μm^2) and is presented as the average number of Prox1 positive nuclei per vessel area ± SEM. The *P* value represents *<0.05 as determined by Student's unpaired t-test.

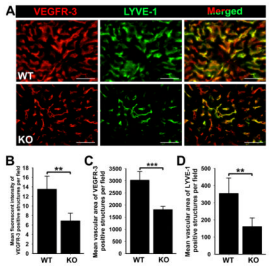

Figure 2.

Deletion of NF-κB p50 KO results in decreased expression of VEGFR-3 and LYVE-1 on liver endothelial cells compared with WT. (**A**) Livers of p50 KO and WT mice were double immunostained with anti-VEGFR-3 and anti-LYVE-1 antibodies, showing decreased VEGFR-3 expression in endothelial cells of p50 KO livers compared with WT. Scale bars represent 50 μm. (**B**) The mean fluorescent intensity of VEGFR-3 staining was analyzed in 3 random fields of p50 KO and WT livers (n = 5 mice per group) at 400X magnification. Data are presented as the mean fluorescent intensity ± SEM. The *P* value represents **<0.01 as determined by Student's unpaired t-test. The mean vascular area of VEGFR-3 (**C**) and LYVE-1 (**D**) positive staining was calculated from 3 independent images of p50 KO and WT livers (n = 5 mice per group). Data are presented as the mean vascular area normalized per total area ± SEM. The *P* values represent **<0.01 and ***<0.001 as determined by Student's unpaired t-test.

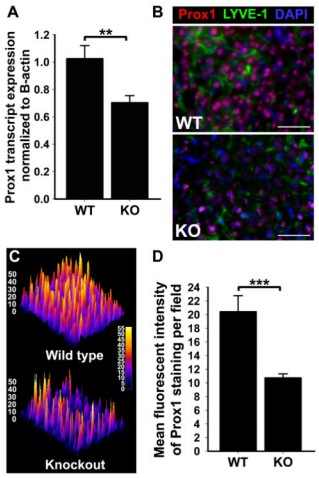

Figure 3.

Expression of Prox1 in the mouse liver is significantly decreased by deletion of NF-κB p50 KO as compared with WT. (**A**) Quantitative RT-PCR analysis of Prox1 transcript expression in total RNA extracted from p50 KO and WT livers (n = 5 mice per group). Relative expression was normalized to β-actin. Data are presented as mean transcript expression ± SEM. *P* values are indicated as *<0.01 as determined by Student's unpaired t-test. (**B**) Liver sections were double immunostained with anti-Prox1 and anti-LYVE-1 antibodies. Scale bars represent 50 μm. (**C**) A representative surface plot of the fluorescent intensity of Prox1 staining in p50 KO and WT liver sections. Note in panels (**B**) and (**C**) a dramatic reduction in Prox1 expression in both liver sinusoidal endothelial cells and hepatocytes. (**D**) The mean fluorescent intensity of Prox1 staining was analyzed in 3 random fields of p50 KO and WT livers (n = 5 mice per group) acquired at 400X magnification. Data are presented as the mean fluorescent intensity± SEM. The *P* value represents ***<0.001 as determined by Student's unpaired t-test.

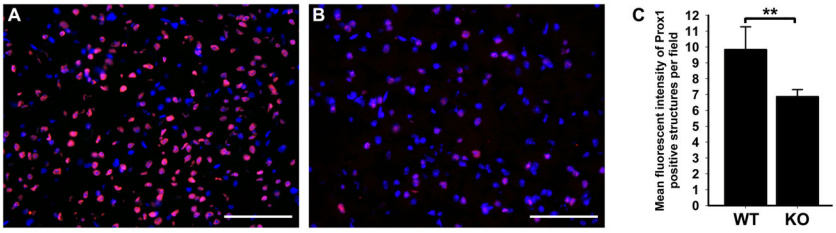

Figure 4.

Cell-type specific downregulation of Prox1 in neurons of p50 KO brains compared with WT. Frozen sections of p50 WT (**A**) and KO (**B**) brains were immunostained with anti-Prox1 antibodies and counterstained with DAPI. Note the dramatic reduction in the fluorescent intensity of Prox1 immunostaining in p50 KO compared with WT. (**C**) Analysis of the MFI of Prox1 staining in p50 KO and WT neurons (n = 3–4 mice per group). Data are presented as MFI of Prox1 staining ± SEM. The *P* value represents **<0.01 as determined by Student's unpaired t-test.

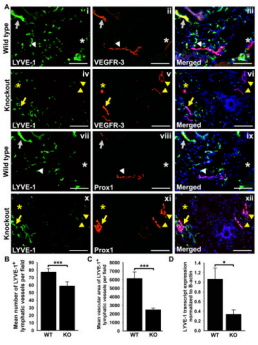

Figure 5.

Decreased LYVE-1$^+$ lymphatic vessel density despite elevated expression of VEGFR-3 and Prox1 in the MFP of p50 KO mice compared with WT. (**A**) Serial frozen sections of p50 KO and WT MFP were double-immunostained with anti-LYVE-1 and anti-VEGFR-3 (i–vi) or anti-LYVE-1 and anti-Prox1 (vii–xi) antibodies. Scale bar represents 100 μm. Some VEGFR-3$^+$/Prox1$^+$ lymphatic vessels also expressed LYVE-1 (arrows), whereas other VEGFR-3$^+$/Prox1$^+$ lymphatic vessels were LYVE-1 negative (arrowhead). Vascular structures resembling blood vessels also stained positive for VEGFR-3 but negative for lymphatic markers Prox1 and LYVE-1 (asterisk). Note that overall density and expression of VEGFR-3$^+$/Prox1$^+$ was increased in p50 KO (iv–vi and x–xii) compared with WT (i–iii and vii–ix). (**B**) LYVE-1positive lymphatic vessels were enumerated in 6 images per p50 KO and WT MFPs (n = 3 mice per group) acquired at 200X magnification. The results are presented as the mean LYVE-1 positive vessel density per 200X field ± SEM. The *P* value represents ***<0.001 as determined by Student's unpaired t-test. (**C**) The mean vascular area of LYVE-1 positive vessels was measured from 3 images of p50 KO and WT MFPs (n = 3 mice per group) acquired at 200X magnification. The *P* value represents ***<0.001 as determined by Student's unpaired t-test. (**D**) Quantitative RT-PCR analysis of LYVE-1 was performed using total RNA extracted from p50 KO and WT MFPs (n = 4–5 mice per group). Relative expression was normalized to β-actin. Data are presented as the mean β-actin normalized transcript expression ± SEM. The *P* value represents *<0.05 as determined by Student's unpaired t-test.

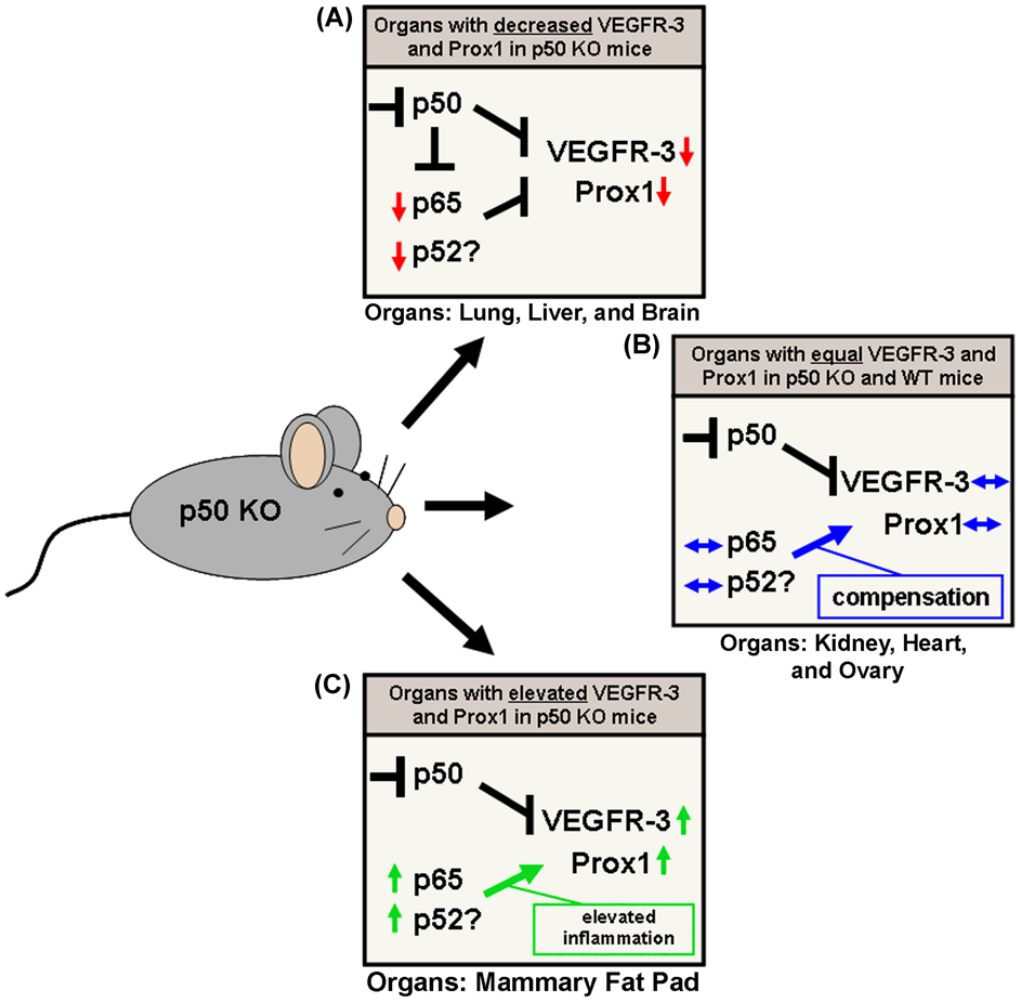

Figure 6.

Potential impact of NF-κB p50 deletion on expression of VEGFR-3 and Prox1. (**A)** Expression of VEGFR-3 and Prox1 was significantly downregulated in several organs of p50 KO mice (e.g. lung, liver, and brain), which correlated with a global reduction of the other major NF-κB transcription factors, p65 and p52. This is consistent with previous findings that several NF-κB subunits are variably downregulated in a cell type-specific manner in different tissues of p50 KO mice [67]. This suggests that p50 along with p65 and p52 might be involved in transcriptional regulation of VEGFR-3 and Prox1 expression. (**B**) In comparison, deletion of NF-κB p50 did not affect expression of NF-κB p65 and p52 in the kidney, heart, and ovary of p50 KO mice, corresponding to equal expression of VEGFR-3 and Prox1 in the same p50 KO organs compared to WT. This suggests that in these organs p50 may be dispensable for regulation of expression of VEGFR-3 and Prox1 and other subunits of NF-κB (e.g., p65 and p52). (**C**) In one p50 KO tissue, the mammary fat pad, the expression of NF-κB p65 and p52 was dramatically increased along with elevated expression of 35 inflammatory cytokines (Table 5). This corresponded to significantly increased levels of VEGFR-3 and Prox1 expression, despite the lack of the p50 subunit of NF-κB. **For both panels B and C:** Since NF-κB p65 and p52 have previously been shown to bind and activate NF-κB p50 response elements (i.e., κB sites), this implies that NF-κB p65 and p52 might potentially compensate or overcompensate for the lack of NF-κB p50 signaling in certain organs. Furthermore, NF-κB p65 was previously shown to

independently regulate the VEGFR-3 promoter and be required for expression of Prox1 in cultured LECs [20], further suggesting that other NF-κB subunits may regulate expression of VEGFR-3 and Prox1 in addition to p50.

Table 1

Sequences of primers used for qRT-PCR

qRT-PCR primers	Primer Sequences	Product size (bp)
VEGFR-3		182
Sense	5′-CTGGCAAATGGTTACTCCATGA-3′	
Antisense	5′-ACAACCCGTGTGTCTTCACTG-3′	
Prox 1		65
Sense	5′-TACCAGGTCTACGACAGCACCG-3′	
Antisense	5′-GTCTTCAGACAGGTCGCCATC-3′	
LYVE-1		112
Sense	5′-CAGCACACTAGCCTGGTGTTA-3′	
Antisense	5′-CGCCCATGATTCTGCATGTAGA-3′	
β-actin		153
Sense	5′-GGCTGTATTCCCCTCCATCG-3′	
Antisense	5′-CCAGTTGGTAACAATGCCATGT-3′	
p65 (Rela)		75
Sense	5′-GCTACAC**G**GGACCAGGAACAG-3′[#]	
Antisense	5′-AGTTCATGTGGATGAGGCCG-3′	
p52 (NF-κB2)		157
Sense	5′-GGCCGGAAGACCTATCCTACT-3′	
Antisense	5′-CTACAGACACAGCGCACACT-3′	
c-Rel		124
Sense	5′-TTGAAGACTGCGACCTCAATG-3′	
Antisense	5′-GGGGCACGGTTATCATAAATTGG-3′	
Relb		157
Sense	5′-CCGTACCTGGTCATCACAGAG-3′	
Antisense	5′-CAGTCTCGAAGCTCGATGGC-3′	

[#]Primer detects both rat and mouse p65 with a one base pair mismatch with the mouse sequence denoted in underlined bold

Table 2

Lymphatic vessel density (LVD) in normal organs of p50 KO and WT mice

	LVD [per mm^2)†			
Organ	**WT**	**KO**	**Percent decrease**	***P*-va lue**
Lung	966 ± 90	585 ± 55′	39.4%	<0.001
Liver	1307 ± 120	1133 ± 83	13.4%	0.05
MFP	1917 ±167	1569 ± 144	18.2%	<0.001
Kidney	11 ± 3	11 ± 2$^{\#}$	0.0%	n.s.‡
Heart	125 ± 9	126 ± 10	0.0%	n.s.
Ovary	1049 ± 104	938 ± 184	10.6%	n.s.

†LVD was calculated from frozen organ sections stained with anti-LYVE-1 antibodies. Note that both LYVE-1^{+} lymphatic and sinusoidal endothelium of the liver were enumerated to calculate hepatic LYVE-1^{+} vessel density. Three independent images were acquired per animal (n = 3–5 mice per group). Data are presented as mean LVD ± SEM.

$^{\#}$LVD was normalized to the tissue circumference

‡n.s. denotes non-significant changes

Table 3

Relative changes in Prox1 and VEGFR-3 expression in normal organs of p50 KO *versus* WT mice

	Prox1				VEGFR-3			
Organ	**qRT-PCR¶**	***P*-value**	**MFI#**	***P*-value**	**qRT-PCR¶**	***P*-value**	**MFI#**	***P*-value**
Lung	56 ± 4%	0.04*	104 ± 5%	n.s.‡	75 ± 10%	n.s.	99 ± 19%	n.s.
Liver	70 ± 5%	0.03	53 ± 3%	<0.001	71 ± 6%	0.004	49 ± 12%	0.002
MFP	243 ± 45%	0.02	123 ± 15	0.05	180 ± 29%	0.05	134 ± 12%	0.001
Kidney	90 ± 13%	n.s.	100 ±9%	n.s.	85 ± 6%	n.s.	100 ±8%	n.s.
Heart	82 ± 15%	n.s.	98 ± 1%	n.s.	96 ± 6%	n.s.	103 ± 6%	n.s.
Ovary	103 ±27%	n.s.	85 ± 5%	0.004	126 ± 42%	n.s.	102 ±9%	n.s.
Brain	49 ± 12%	0.01	75 ± 3%	0.01	109 ± 8%	n.s.	—	—

¶Transcript expression analyzed by qRT-PCR and presented as the percent expression in p50 knockouts compared with wild type control mice (n = 3–5 mice per group)

#Mean fluorescent intensity (MFI) presented as the percent expression in p50 knockouts compared with wild type control mice (n = 3–5 mice per group)

**P* value was determined by Student's unpaired t-test

‡n.s. denotes non-significant changes

Table 4

Relative expression of Prox1 and VEGFR-3 transcripts compared to expression of NF-κB p65 and p52 subunits in p50 KO *versus* WT mice

Tissue†	*Prox1*	*VEGFR-3*	*p65 (Rela)*	*P*	*p52 (NF-κB2)*	*P*
Lung	56 ± 4%	75 ± 10%	58 ± 5%	<0.001	57 ±10%	0.05
Liver	70 ± 5%	71 ± 6%	79 ± 2%	0.002‡	76 ± 5%	0.05
MFP	243 ± 45%	180 ± 29%	140 ± 4%	0.001	158 ± 2%	0.005
Kidney	90 ± 13%	85 ± 6%	100 ± 6%	n.s.¶	88 ±10%	n.s.
Heart	82 ± 15%	96 ± 6%	90 ± 3%	0.03	69 ± 2%	<0.001
Brain	49 ± 12%	109 ± 8%	97 ± 7%	n.s.	76 ± 5%	0.03

† cDNA synthesized from total RNA extracted from each tissue (n = 3–5 mice per group)

‡ *P* value was determined by Student's unpaired t-test

¶ n.s. denotes non-significant changes

Table 5

Changes in expression of inflammatory mediators in MFPs of p50 KO *versus* WT mice

Gene name	Symbol	Fold change compared with WT	Gene name	Symbol	Fold change compared with WT
Interleukin 17B¶	Il17b	9.25‡	Chemokine (C-C motif) ligand 20	Ccl20	1.16
Complement component 3	C3	6.06	Interleukin 4	Il4	1.16
Chemokine (C-C motif) receptor 10	Ccr10	5.86	Interleukin 16	Il16	1.14
Tumor necrosis factor receptor superfamily, member 1a	Tnfrsf1a	4.72	Chemokine (C-C motif) ligand 17	Ccl17	1.12
			Interferon gamma	Ifng	1.10
Macrophage migration inhibitory factor	Mif	3.89	Chemokine (C-C motif) ligand 24	Ccl24	1.10
Interleukin 13 receptor, alpha 1	Il13ra1	3.61	Chemokine (C-C motif) receptor 9	Ccr9	1.09
Small inducible cytokine subfamily E, member 1	Scye1	3.27	Interleukin 1 alpha	Il1a	1.07
			Chemokine (C-C motif) ligand 19	Ccl19	1.06
Interleukin 6 signal transducer	Il6st	3.12	Chemokine (C-C motif) receptor 4	Ccr4	1.06
Interleukin 18	Il18	2.83	Chemokine (C-X-C motif) ligand 5	Cxcl5	1.06
ATP-binding cassette, sub-family F (GCN20), member 1	Abcf1	2.73	Chemokine (C-C motif) ligand 3	Ccl3	1.01
			Interleukin 1 receptor, type II	Il1r2	1.00
Chemokine (C-X-C motif) ligand 15	Cxcl15	2.68	Chemokine (C-C motif) receptor 2	Ccr2	0.93
Chemokine (C-C motif) ligand 11	Ccl11	2.62	Chemokine (C-C motif) ligand 6	Ccl6	0.90
B-cell leukemia/lymphoma 6	Bcl6	2.60	Chemokine (C-C motif) ligand 9	Ccl9	0.88
Chemokine (C-X3-C motif) ligand 1	Cx3cl1	2.60	Interleukin 10 receptor, alpha	Il10ra	0.87
Chemokine (C-C motif) receptor 5	Cxcr5	2.51	Chemokine (C-C motif) ligand 7	Ccl7	0.84
C-reactive protein, pentraxin-related	Crp	2.50	Integrin alpha M	Itgam	0.81
Chemokine (C-X-C motif) ligand 12	Cxcl12	2.28	Chemokine (C-C motif) ligand 2	Ccl2	0.77
Interleukin 15	Il15	2.27	Interleukin 1 beta	Il1b	0.76
Secreted phosphoprotein 1	Spp1	2.17	Chemokine (C-C motif) ligand 4	Ccl4	0.69
Interleukin 1 receptor, type I	Il1r1	1.93	Chemokine (C-C motif) ligand 12	Ccl12	0.66
Interleukin 1 family, member 8	Il1f8	1.85	Chemokine (C motif) receptor 1	Xcr1	0.64
Chemokine (C-C motif) receptor 1	Ccr1	1.80	Integrin beta 2	Itgb2	0.62
Chemokine (C-X-C motif) ligand 9	Cxcl9	1.74	Interleukin 5 receptor, alpha	Il5ra	0.60
Interleukin 11	Il11	1.74	Chemokine (C-C motif) ligand 1	Ccl1	0.59
Transforming growth factor, beta 1	Tgfb1	1.74	Chemokine (C-X-C motif) ligand 1	Cxcl1	0.59

Gene name	Symbol	Fold change compared with WT	Gene name	Symbol	Fold change compared with WT
Chemokine (C-X-C motif) ligand 10	Cxcl10	1.71	Interleukin 8 receptor, beta	Il8rb	0.59
Chemokine (C-X-C motif) ligand 11	Cxcl11	1.69	Interleukin 10	Il10	0.48
Interleukin 6 receptor, alpha	Il6ra	1.69	Chemokine (C-X-C motif) receptor 3	Cxcr3	0.45
Toll interacting protein	Tollip	1.69	Interleukin 3	Il3	0.39
Caspase 1	Casp1	1.68	Interleukin 2 receptor, beta chain	Il2rb	0.37
Tumor necrosis factor receptor superfamily, member 1b	Tnfrsf1b	1.65	Chemokine (C-X-C motif) ligand 13	Cxcl13	0.36
			Chemokine (C-C motif) receptor 8	Ccr8	0.28
Platelet factor 4	Pf4	1.61	Lymphotoxin A	Lta	0.24
Chemokine (C-C motif) ligand 8	Ccl8	1.59	Chemokine (C-C motif) receptor 7	Ccr7	0.24
Interleukin 10 receptor, beta	Il10rb	1.57	Interleukin 2 receptor, gamma chain	Il2rg	0.16
Chemokine (C-C motif) receptor 3	Ccr3	1.51	Chemokine (C-C motif) receptor 6	Ccr6	0.16
Tumor necrosis factor	Tnf	1.49	Chemokine (C-C motif) ligand 5	Ccl5	0.13
Chemokine (C-C motif) ligand 25	Ccl25	1.43	Chemochine (C-X-C motif) receptor 5	Ccr5	0.12
Interleukin 13	Il13	1.38	Lymphotoxin B	Ltb	0.07
Interleukin 20	Il20	1.27	CD40 ligand	Cd40lg	0.05
Interleukin 1 family, member 6	Il1f6	1.26	Chemokine (C-C motif) ligand 22	Ccl22	0.04

‡Fold changes were derived from qRT-PCR array analysis of total MFP mRNA from p50 KO and WT mice (n = 4 mice per group)

¶Gray shading indicates genes with greater than 0.5-fold change expression in p50 KO compared with WT MFP